Journal of Environmental Management 339 (2023) 117884

Contents lists available at ScienceDirect

Journal of Environmental Management

journal homepage: www.elsevier.com/locate/jenvman

Research article

Magnetic separation for arsenic and metal recovery from polluted sediments within a circular economy

D. Baragaño [a,b,*], E. Berrezueta [c], M. Komárek [b], J.M. Menéndez Aguado [a]

[a] Department of Mining Exploitation and Prospecting, Campus of Mieres, University of Oviedo, Mieres, 33600, Mieres, Asturias, Spain
[b] Department of Environmental Geosciences, Faculty of Environmental Sciences, Czech University of Life Sciences Prague, Kamýcká 129, 165 00, Prague, Suchdol, Czech Republic
[c] Spanish Geological Survery (IGME-CSIC), Matemático Pedrayes, 25, 33005, Oviedo, Spain

ARTICLE INFO

Keywords:
Sediments
Magnetic separation
Remediation
Arsenic
Metals
Circular economy

ABSTRACT

Several metals and metalloids (e.g., As, Cd, Cu, Pb, Zn) are toxic at low concentrations, thus their presence in sediments can raise environmental concern. However, these elements can be of economic interest, and several techniques have been used for their recovery and some of them have been widely applied to mining or to industrial soils, but not to sediments. In this work, wet high-intensity magnetic separation (WHIMS) was applied for As, Cd, Cu, Pb and Zn recovery from polluted sediments. A composite sample of 50 kg was taken in the Avilés estuary (Asturias, North Spain) with element concentrations above the legislation limits. Element distribution was assessed using wet-sieving and ICP-MS analysis, revealing that the 125–500 μm grain-size fraction accounts for the 62 w% of the material and that element concentration in this fraction is lower than in the other grain size fractions. Subsequently, WHIMS was applied at three different voltage intensities for the 125–500 μm and <125 μm fractions, revealing excellent recovery ratios, especially for the coarser material. Furthermore, magnetic property measurements coupled to microscopy analysis revealed that the success of the technique derives from concentrating metal-enriched iron oxides particles (ferro- and para-magnetic material) in a mixture of quartz and other minerals (diamagnetic particles). These results indicate the feasibility of the magnetic separation for metal and metalloid recovery from polluted sediments, and thus offer a double benefit of coastal area restoration and valuable material recovery in the context of a circular economy.

1. Introduction

Coastal areas have great ecological value and economic importance as they are home to several autochthonous plants and animals, including numerous migratory birds, several species of fish, and a considerable number of mammals (Anbuselvan et al., 2018; Jha et al., 2019). Moreover, coastal areas offer favourable conditions for the industry and human settlements due to the abundance of fresh water and fertile land, inexpensive transportation facilities by ship, and their potential for tourism and recreational activities (Mossinger et al., 2013). These features have made them preferred places for human settlement and, thus, they are frequently drastically altered by industrial activities, navigation, agriculture, and municipal uses, even waste disposal (Kennish, 2002, 2017). These activities may affect sediment quality, interfering with wildlife and even posing a threat to human health. Several types of pollutants - including metals and metalloids - can be present in coastal environments.

Some metals and metalloids (e.g., As, Cd, Cu, Pb, Zn) are toxic even at low concentrations (Li et al., 2022; Xu and Fu, 2022). Although they exist naturally in the Earth's crust, their presence is often a consequence of anthropogenic activities such as mining and industry (Liu et al., 2020; Wu et al., 2018). These elements can be released to different environmental compartments from natural or anthropogenic sources (Xu et al., 2015), such as industrial emissions, coal combustion, non-ferrous metal production, or mining activities (Fernández et al., 2020; Forján et al., 2019). Their accumulation in these environments can cause loss of wildlife habitats, biomagnification, degradation of plankton populations, and it can even affect human health by direct exposure or by the consumption of contaminated animals (Li et al., 2020). Therefore, their presence in sediments pose a severe risk for human health and the environment due to their non-degradative nature, persistence, and long-term effects.

* Corresponding author. School of Mines and Energy Engineering, University of Cantabria, Blvr. Ronda Rufino Peón 254, 39300 Torrelavega, Cantabria, Spain.
E-mail address: diego.baragano@unican.es (D. Baragaño).

https://doi.org/10.1016/j.jenvman.2023.117884
Received 4 January 2023; Received in revised form 17 February 2023; Accepted 4 April 2023
Available online 16 April 2023

To resolve the problems associated with polluted sediments, several treatment technologies have been developed over the last decades, such as dredging, in situ immobilisation, capping methods, chemical injection, physical separation, thermal treatments, or biological technologies (Gao et al., 2021; Mulligan et al., 2001a; Wang et al., 2018). The most common treatment is sediment dredging, although, when the sediments cannot be reused, they are disposed of in landfills (Norén et al., 2020). Moreover, dredging is an essential technique to maintain proper water depths in ports (Crocetti et al., 2022). To diminish the size of these landfills, alternative treatments have been studied. Physical separation was found to be a cleaner way of polluted sediment management, reducing the quantity of polluted materials (Mulligan et al., 2001b; Peng et al., 2009). Furthermore, with increasing metal prices, higher landfill costs, and cheaper metal recovery techniques, the metal extraction from polluted sediments is an opportunity to recover valuable metals, it contributes to a circular economy, and reduces the need for their mining (Norén et al., 2020; Pell et al., 2021).

Although several physical separation processes have been used for cleaning polluted sediments, mainly screening (Peng et al., 2009), flotation (Cauwenberg et al., 1998), ultrasonic-assisted extractions (Kyllönen et al., 2004; Meegoda and Perera, 2001) or hydrocyclones (Mulligan et al., 2001a, 2001b), magnetic extraction has not been successfully applied so far (Akcil et al., 2015; Mulligan et al., 2001a). However, this approach has been effectively tested in soil remediation (Baragaño et al., 2021; Dermont et al., 2008; Sierra et al., 2014b). In this context, the main objective of this work is to test the feasibility of high-intensity magnetic separation for recovering arsenic and metals from a polluted sediment using geochemical, mineralogical and magnetic tools.

2. Methodology

2.1. Site description and sampling

Avilés has been one of the most important industrialized areas in the north of Spain (Gallego et al., 2002). Metallurgical industries that have been operating in the area affected air (Negral et al., 2020), soil (Sierra et al., 2014a) and sediment (Baragaño et al., 2021) quality for decades. The sampling area for this study (Fig. S1) was located on the left bank of the River of Avilés, in the surroundings of a Zn smelter, where sediment samples revealed metal (loid) contamination exceeding Sediment Screening Levels (SSLs) (Baragaño et al., 2021). This area is part of the San Juan de Nieva beach and the El Espartal dune system, which is the largest aeolian dune system of Asturias (Flor-Blanco et al., 2013) and was declared a Natural monument in 2006 (CMAOTI, 2006). The characteristic sediment of the area is a medium sand formed by the fragmentation of the Triassic siltstone, Jurassic limestone, and Middle Jurassic siliceous conglomerate (Flor-Blanco et al., 2013; Julivert et al., 1973). To perform the experiments, a bulk sediment sample of about 50 kg was collected. A composite sample was generated by several subsamples covering the whole area where As and several metals were detected at higher concentrations.

2.2. Sediment characterization and wet sieving

The sediment sample was homogenised and representative subsamples were obtained by wet sieving of the particle-size fractions of <125, 125–500, 500–2000 and > 2000 μm. Standard sieves were placed in a column, and batches of 100 g of the material were placed in a sieve shaker for 5 min with a water flow of 0.3 l/min (ASTM D-422-63, Standard Test Method for Particle-Size Analysis). Fractions were then dried at 30 °C to prevent chemical alterations and weighed.

To standardize the conditions used for chemical analysis, samples of >125 μm were ground in a RS100 Resch mill at 400 rpm for 40 s. Then, 1 g of the different representative subsamples (i.e., bulk sample, different grain-size fractions, etc.) was subjected to acid digestion. The total concentrations of As, Cd, Cu, Fe, Hg, Pb, and Zn in the digested material were determined by Inductively Coupled Plasma-Optical Emission Spectroscopy (ICP-OES) at the accredited (ISO 9002) Bureau Veritas Laboratories (Vancouver, Canada).

Furthermore, a preliminary mineralogical analysis of milled samples was obtained by X-Ray diffraction analysis (XRD). Powder X-Ray diffraction (PXRD) patterns were measured on a PANalytical X'Pert Pro MPD diffractometer with Cu kα1 radiation (1.540598 Å) to determine the mineralogical composition. After determining the position of Bragg peaks observed over the range of 2θ = 5–90°, the minerals were identified using databases of the International Centre for Diffraction Data.

2.3. Wet high-intensity magnetic separation

For the finer fractions, dry magnetic separation is not effective. When soil particles are extremely fine (even <63 μm), wet high-intensity magnetic separation (WHIMS) is a suitable technique that can separate paramagnetic and non-magnetic materials and avoids dust generation. In this work, the OUTOTEC Laboratory WHIMS 3X4L was used. Feed sediment samples were prepared previously by mixing 50 g of the grain size fraction of <125 or 125–500 μm with 200 g of water. Then, the pulp was fed into the apparatus passing through a matrix canister filled with magnetized steel spheres 12.7 mm in diameter; this is where the separation occurs. The sediment mixture retained in the matrix represented the magnetic fraction (MF), while the non-magnetic fraction (NMF) passed through the matrix and was collected in a pan. Finally, the magnetic field was reduced to zero, and the MF was obtained by washing the spheres. The magnetic voltages used in the tests were 10, 30 and 50% of the maximum output voltage. After separation, both MF and NMF samples were air-dried and, subsequently, subjected to chemical analysis (described in the previous section) and magnetic analysis.

2.4. Metallurgical efficiency and general economic assessment

The results of chemical analysis obtained from the magnetic separations were used to evaluate the effectiveness of the processes. Firstly, from a technical point of view, we determined the weight recovery (WR) defined as the percentage of material of each fraction (i.e., MF and NMF) with respect to the feed material (Wills and Napier-Munn, 2006). For the MF fraction, WR is calculated using the following expression:

$$WR_{MF} = \frac{m_{MF}}{m_{MF} + m_{NMF}} \bullet 100 \quad (1)$$

Where m_{MF} and m_{NMF} are the masses of sediment of both fractions, MF and NMF respectively, in grams. Likewise, WR_{NMF} can be calculated as the difference between 100 and WR_{MF}, as expressed in the following formula:

$$WR_{NMF} = 100 - WR_{MF} \quad (2)$$

Secondly, element recovery (ER) was calculated for each element. It can be defined as the percentage of the amount of the element in each fraction with respect to the amount of the element in the feed material. For example, in case of element recovery in MF, the ER is calculated according to the following formula:

$$ER_{MF} = \frac{WR_{MF} \bullet c_{MF}}{(WR_{MF} \bullet c_{MF}) + (WR_{NMF} \bullet c_{NMF})} \quad (3)$$

Where c_{MF} and c_{NMF} are the element concentrations in the separated fractions, MF and NMF respectively. Similarly to WR, this parameter can be also determined for the NMF:

$$ER_{NMF} = 100 - ER_{MF} \quad (4)$$

Then, both parameters were plotted on a graph to compare the separations for all the studied elements.

Finally, Fe concentration was used to evaluate the magnetic sepa-

ration due to its usual ferromagnetic contribution to the particles. Thus, a separation efficiency parameter was determined according to the following formula (Chen, 2011):

$$E = WR_{MF} \bullet \left(1 - \frac{[Fe]_F \bullet ([Fe]_H)}{[Fe]_{MF} \bullet ([Fe]_H - [Fe]_F)}\right) \quad (5)$$

where, $[Fe]_F$ and $[Fe]_{MF}$ are the Fe concentration in the feed and MF respectively, and $[Fe]_H$ is the maximum iron concentration of hematite (70% Fe). Note that Fe concentration is expressed in percentage, thus E is within the range of 0–100.

On the other hand, the feasibility of the approach has been also tested from an economical point of view. In this sense, three different scenarios were compared to determine the economic impact of the magnetic separation during the site restoration process. In the first scenario, the economic cost of excavation and transport of the contaminated material to a waste landfill was determined, taking into account real data provided by private companies from the region to calculate the operational costs of the restoration actions. In the second scenario, the cost of the magnetic separation technique and the transport of the magnetic fraction to the waste landfill is incorporated, along with the associated costs. In the last scenario, the second one is modified to eliminate the transport of the polluted material to the landfill, and the revaluation is estimated to recover the Zn present in this material.

2.5. Magnetic characterization

WHIMS uses the most intense magnetic field among the experiments, thus it makes it possible to separate the ferro-, ferri- and paramagnetic particles from the diamagnetic ones. To evaluate the separation, magnetic hysteresis loops were obtained for the feed sediment and sediment fractions (MF and NMF) obtained by WHIMS using a Microsense EV9 vibrating sample magnetometer (VSM). The magnetization (M) was measured as a function of the magnetic field (H) in a complete cycle between 20 kOe and −20 kOe at room temperature.

The saturation magnetization (σ_s) and the high-field susceptibility (κ) of each sample were determined by fitting the measured data of the high-magnetic field region (5–20 kOe) according to the following expression (Baragaño et al., 2021):

$$\sigma = \sigma_S\left(1 - \frac{a}{H} - \frac{b}{H^2}\right) + \kappa H \quad (6)$$

2.6. Mineralogical approach and electron microprobe

After the chemical analysis, the magnetic fractions (MF) were selected for a mineralogical and petrographic study, which formed the basis of the characterization process and made it possible to identify the pollutant bearing phases. An OpM (Leica DM 6000 polarization microscope), a SEM (JEOL JSM-5600 SEM, using W-Filament, acceleration voltage of 20 kV and Inca Energy-200 software) and a Cameca SX-100 electron microprobe (EMPA) equipped with five WDS spectrometers and one EDS spectrometer were used. All the experimental runs and studies were performed at the Geological Survey of Spain and at the University of Oviedo.

3. Results and discussion

3.1. Sediment and grain-size characterization

The ICP-OES analyses revealed that As, Cd, Cu, Pb and Zn concentrations in the sediment exceed the Probable Effect Levels (PELs) established by the Canadian Guidelines for Protection of Aquatic Life (Table 1), indicating adverse effects on biota (CCME, 2001). Furthermore, Table 1 summarizes the results of the grain-size analysis for the three obtained fractions, as well as the element concentrations in each of them. The finest (<125 μm) and the coarsest (500–2000 μm) fractions represent the 38 w% of the material, while the 62 w% is formed by particles from the 125–500 μm grain-size fraction. Therefore, the <125 μm and 125–500 μm fractions were selected for WHIMS experiment since the 500–2000 μm fraction only represents 8 w% of the material. Pollutant concentrations were high in the finest grain-size fraction, and high concentrations were also found in the coarse grain-size fraction. On the other hand, the screening of the sediment revealed that a great amount of material (the 125–500 μm fraction, which is 62 w% of the total) did not present significant As, Cd, Cu, Pb and Zn concentrations, although their concentration values were still slightly higher than PELs, with the exception of Cu.

Pollutant distribution indicates that different materials were mixed in the study area (Baragaño et al., 2022). These materials included sand from the beach (with a grain-size distribution of 125–500 μm), slag particles with large grain sizes, and finer particles probably deposited from dust emission. It is also noteworthy that Fe content in the polluted grain-size fractions (i.e., the 500–2000 μm and the <125 μm fractions) is considerably higher than in the unpolluted fraction (125–500 μm), which suggests that the pollutants are probably linked to Fe-enriched particles, and therefore to ferromagnetic particles of the sediment.

Regarding sediment mineralogy, XRD patterns of the <125 and 125–500 μm fractions (Fig. 1) reveal similar composition. Quartz and glauconite are the main mineral phases, although their concentration is higher in the 125–500 μm fraction than in the one <125 μm. Both phases are minerals typically found in marine sedimentary environments (Nukazawa et al., 2021; Wang et al., 2018). Secondary minerals are calcite and fluorspar; iron oxide, dolomite, and Zn–Mn iron oxide were identified in minor amounts. Other detected chemical products are calcium arsenide and lead hydroxide, which might come from the Zn smelter close to the site (Baragaño et al., 2022). Taking XRD results into account, and in accordance with Fe concentrations, the feasibility of the magnetic separation looks promising since ferromagnetic materials, such as iron oxides, could be easily separated from the main phases, i.e., quartz and glauconite (diamagnetic materials).

3.2. Metallurgical accounting

For a chemical evaluation of the magnetic separation, the separation

Table 1
Grain size distribution and element concentration of the bulk and initial grain-size fractions. PEL = Probable Effect Levels (CCME, 2001). Results are the average values of three measurements with a standard error < 5%.

Element	Unit	Detection limit	Bulk sediment	Grain-Size fractions			PEL
				500–2000	125–500	<125	
WRc	%		100	8	62	30	
As	ppm	2	142	398	54	141	41.6
Cd	ppm	0.5	18.9	17	6.6	41.1	4.21
Cu	ppm	1	132	70	61	292	108
Fe	%	0.01	2	3	0.95	3.18	
Pb	ppm	2	469	575	149	960	112
Zn	ppm	2	5100	1851	1840	12,700	271

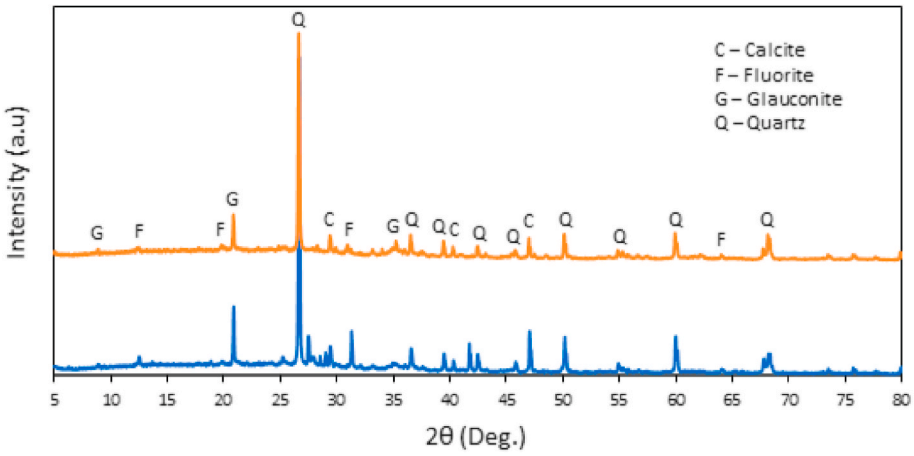

Fig. 1. X-ray diffraction patterns of the polluted sediment of grain size 125–500 μm (blue) and <125 μm (orange). Characteristic peaks of main crystalline phases are shown: quartz (Q), glauconite (G), calcite (C), and fluorspar (F).

efficiency parameter was determined using the Fe concentration. The results are shown in Table 2. Higher values were obtained for the 125–500 μm fraction than for the <125 μm fraction, which suggests that magnetic separation works better for the medium-size particles. XRD revealed a higher percentage of quartz in this grain-size fraction, thus Fe-bearing particles could be easily separated and reported to the MF. Comparing different applied intensity levels, separation efficiency increased with increasing voltage. The greatest change was observed in both fractions when increasing voltage from 10% to 30% due to the strong influence of the intensity on the Fe recovery (Table 2).

In order to assess As and metal recovery, weight recovery and element recovery of the MF were determined for each element, and values were plotted in Fig. 2. As expected, weight recovery (WR) increased with increasing voltage (Fig. 2), thus more ferro- or para-magnetic particles were reported to the MF. However, WR was lower for all separations performed on the 125–500 μm fraction, which is in accordance with the higher amount of quartz in this grain-size fraction.

Fig. 2 reveals two clusters that are clearly separated according to grain-size, and, thereby, indicates that this parameter had a strong effect on the separation. Comparing As and metal recovery (ER values) to Fe recovery, a similar performance was revealed for the finest particles (<125 μm fraction). ER drastically increased for all elements with the voltage intensity change from 10% to 30%, but not with the change to 50%. This suggests that these elements are linked to the same Fe enriched mineral phases, thus come from the same pollution source. On the other hand, element recovery showed a different trend for the 125–500 μm fraction (Fig. 2). When increasing the voltage intensity, Fe recovery increased progressively, but the trends of other metal recoveries varied. For example, As recovery was similar to Fe recovery at 10% and 30% voltage intensity, showing that probably As associated with the MF was linked to Fe-bearing particles. However, at the highest voltage intensity, As recovery decreased compared to the values obtained at lower voltage intensities. Thus, Fe-bearing particles were added to the MF, as revealed by the increase in Fe recovery, but these particles were not enriched in As, thus the As concentration in the MF was reduced by dilution. Therefore, when increasing the voltage intensity higher than 30%, not only anthropogenic particles were reported to the MF, but also geogenic particles without As content.

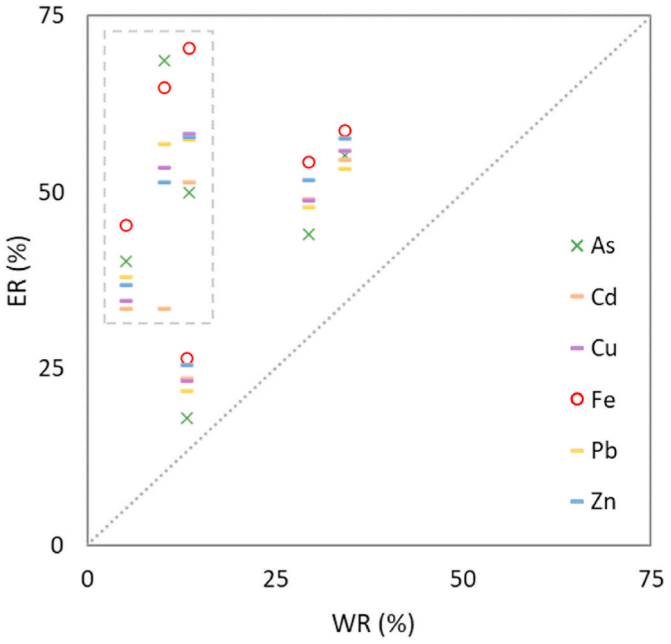

Fig. 2. Element recovery vs. weight recovery for MF after WHIMS. Samples inside the grey box correspond to the 125–500 μm fraction, and the others correspond to the <125 μm fraction. Vertical alignments, from left to right, indicate increasing output voltages.

Table 2
Iron concentration, Fe recovery and separation efficiency for each magnetic separation.

Soil fractions	125–500 μm			<125 μm		
Voltage (%Vmax)	10	30	50	10	30	50
Fe concentration (%)	7.04	4.87	4.40	5.91	5.34	4.79
Fe recovery (%)	45.3	64.9	70.4	26.5	54.4	58.8
Separation efficiency (%)	39.7	52.9	55.9	12.8	23.0	20.7

From an environmental perspective, the 125–500 μm fraction was successfully remediated, since pollutant concentration in the NMF was decreased below PEL values for As, Cd, Cu and Pb, and the amount of material corresponds to 95% of the sediment (Table S1). However, Zn concentration was not reduced below the PEL value, although it was decreased to the 57% of the initial concentration in the feed material (from 1840 to 780 mg/kg). Similar trends were detected for the particles <125 μm, although the decrease in the NMF was not sufficient to reveal concentrations below PEL values, even at the highest voltage, which provided the best results. Moreover, the amount of material reported to the NMF was lower than for the 125–500 μm fraction, thus the remediation approach was ameliorated.

3.3. Separation assessment according to magnetic quantification

Fig. 3 shows hysteresis loops obtained from magnetic measurements for the feed sediment (both grain size fractions, <125 and 125–500 μm) and the magnetic and non-magnetic soil fractions (MF and NMF). Based on the hysteresis loop patterns, ferromagnetic behaviour was detected in the <125 μm fraction of the feed material, while the 125–500 μm fraction showed diamagnetic behaviour (Fig. 3). The saturation magnetization of the <125 μm fraction was around 0.25 emu/g (Table S2), however, this value dropped to 0.04 emu/g in case of the 125–500 μm fraction, suggesting that higher percentage of ferromagnetic particles are present among the finest particles of the sediment.

Considerable differences were detected between the two grain-size fractions. The <125 μm fraction of both MF and NMF (Fig. 3a-b) revealed a ferromagnetic material pattern; however, the 125–500 μm fraction of NMF showed a diamagnetic material pattern (Fig. 3c), in accordance with the chemical analysis (see Fe concentration described above). In this sense, the magnetic characterization suggests that in the coarse material, the metal (loid) source is mainly anthropogenic, with a high affinity to Fe particles. Therefore, when magnetic separation was applied, the geogenic quartz particles from the beach and dunes area were reported to the NMF, showing the distinctive diamagnetic pattern. Increasing the separation voltage, higher volume of ferro- and paramagnetic particles were reported to the MF, thus saturation magnetization was decreased due to dilution effects. On the other hand, lower differences were found regarding NMF when separation voltage was increased.

3.4. Mineralogical analysis of magnetic fraction

The study of the magnetic fractions revealed the presence of As, Cu, Pb, and/or Zn enriched particles (Fig. 4). Although the bulk composition was given by common silicates and oxides (XRD characterization, see section 3.1) that are rather resistant to leaching, the presence of sulphur, such in sphalerite particles (Fig. 4a), indicated a potential increase of the solubility of these metals. The sphalerite found in MF probably comes from the feed material used in the Zn smelter located close to the sampling area. After a more detailed analysis, hematite was found around the particles, probably produced by oxidation and alteration of the sphalerite surface. Moreover, chalcopyrite inclusions were observed, which justifies the presence of Cu in the samples. These types of sulphurs, recovered by the magnetic separation, are a potential source for metal recovery by secondary metallurgical processes.

Regarding the As source, some aggregates of particles were found with higher contents of As, Fe, O and S. We hypothesize that As-enriched sulphurs, such as arsenopyrite, had been present in the mineral paragenesis of the Zn smelter feed material, and, after metallurgical processing, these particles were oxidized. Finally, Pb oxide particles were also found (Fig. 4b) that might have been produced during the Zn metallurgical processes, since low S content was detected, but Zn concentrations were significant (Table 3).

3.5. Applicability, advantages and limitations

Magnetic separation is applicable for recovering metal-bearing particles from soils and sediments when the difference in magnetic properties between these particles and non-polluted particles are significant. In case of non-polluted sediments, the technique is not appropriate since the sediment matrix is heterogeneous and metals of interest are not usually associated with the ferromagnetic materials (Dermont et al., 2008). On the other hand, the recovery of metals is suitable for highly polluted sediments using magnetic separation, although some limitations could be presented on the large-scale applications. Mainly, the treatment system requires large spaces for its operation because the volume of material to be treated must be large to be economically feasible (ITRC, 1997). However, the technology drastically reduces the

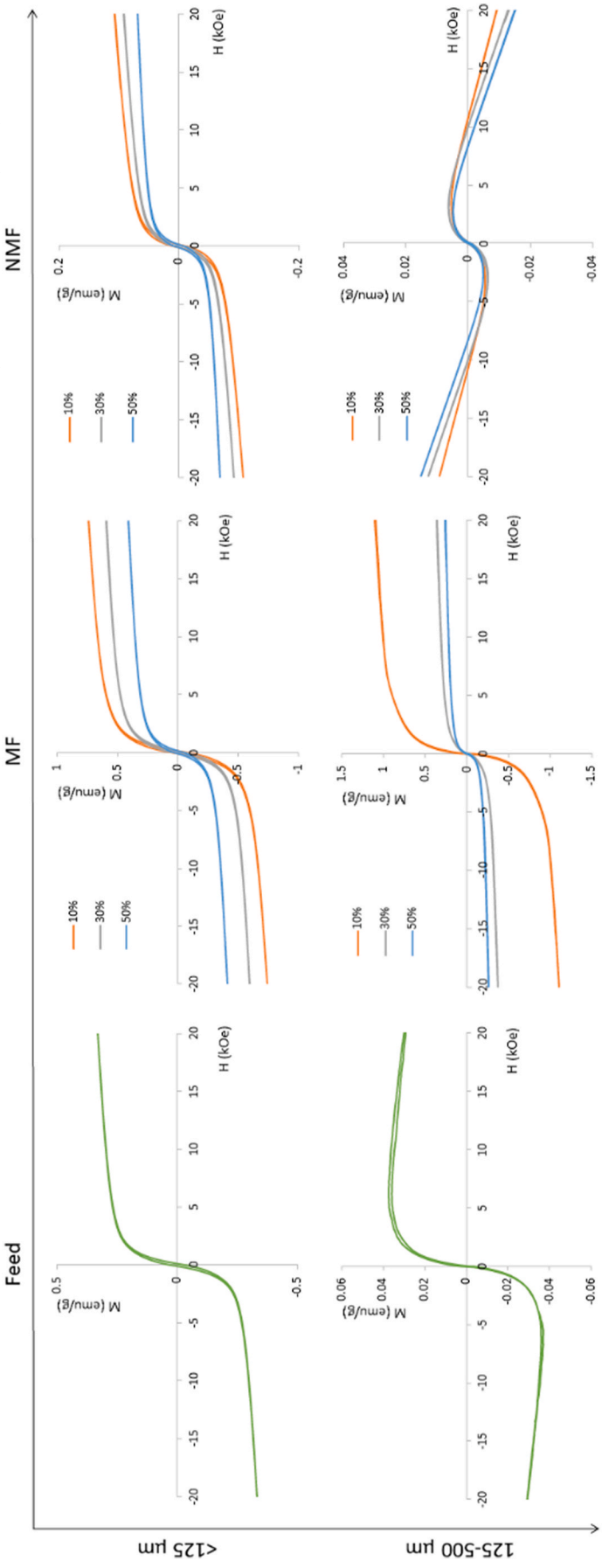

Fig. 3. Hysteresis loops for the feed, MF and NMF. Loops obtained for different separation voltages are represented by different colours: orange (10% Vmax), yellow (30% Vmax) and grey (50% Vmax).

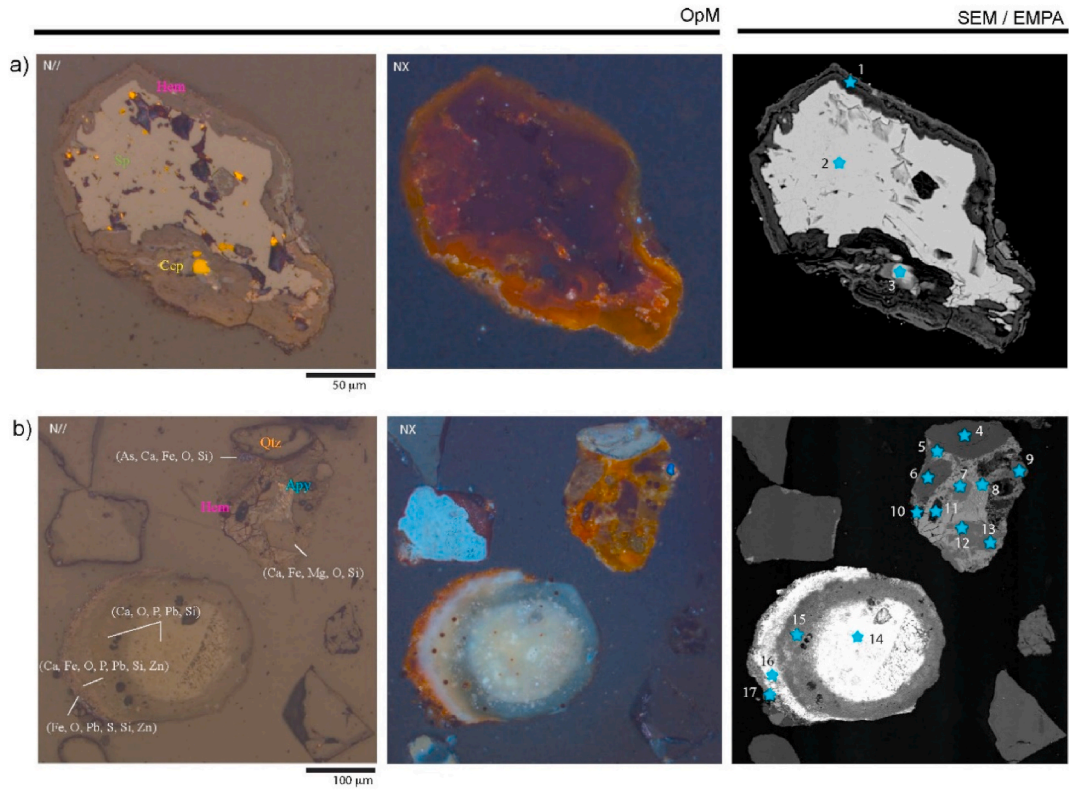

Fig. 4. Optical microscope and SEM photomicrographs and analysis points for EMPA.

Table 3
Element concentrations determined using EMPA for the points marked in Fig. 4.

ID	As	Al	Ba	Ca	Cd	Cu	Fe	K	Mg	Mn	Na	O	P	Pb	S	Si	Sr	Zn
1	0.08		0.08	0.81			65.5					28.5	0.13	1.03	0.08			2.12
2					1.02		3.21					1.32		2.41	26.5			62.1
3						28.6	30.3								28.8			
4							0.08					51.8				45.5		
5	27.0	23.9	0.52	5.82			20.5	0.16			0.14	16.7	0.29			0.92	0.20	2.05
6	0.38	38.6		0.77			4.02	3.89	0.87		0.37	27.1	0.17			20.8		0.45
7				8.67			19.1		4.85	0.28		39.8	0.38			24.0		
8	21.7		0.09	1.25		0.71	37.7					25.7	0.08		9.49	2.32		0.67
9		6.51		18.4			2.85		7.77		0.12	38.6	0.75			21.7		
10	1.72	23.2		0.7			1.58	0.09			0.17	37.3	0.1	0.12		31.3		0.20
11	5.24		0.18	1.92			63.2					25.5	0.55	0.08	0.37	3.20		0.69
12				8.15			17.4		5.76	0.35	0.16	39.9	0.34			24.2		
13	24.9	26.3	0.31	1.74		0.56	24.9					16.8	0.10			0.78	0.11	0.72
14	0.06	14.2		10.9	0.11	0.05	0.11				0.16	14.7	7.26	50.1		0.09		0.62
15	0.19	35.0		2.37	0.09	0.17	5.79	1.09	0.18	0.14	0.06	12.8	1.83	26.1		4.65		6.87
16	0.48	19.3		0.35		0.37	2.40	0.23	0.33	0.23	0.52	19.0	0.09	29.5	1.37	2.86		18.2
17	0.06	27.8		1.34		0.27	21.1	0.18	0.17	0.28	0.94	17.5	0.52	7.18	4.69	3.44		12.3

Only values higher than 0.05% are shown.

volume of polluted sediment and favours the possibility for metals recovery. In this sense, an analysis of the feasibility of the magnetic separation application over the study site was assessed.

In 2001, an area located on the left bank of the Avilés Estuary was restored for improving the chemical quality of the San Juan de Nieva beach and dunes (Baragaño et al., 2021). During this activity, 180,000 m^3 of polluted sediments were excavated, transferred and deposited on a hazardous waste landfill, and a sandy refill from a nearby submarine deposit was used for completing the restoration. Taking into account the average density of the polluted sediments, 2.65 t/m^3, 477,000 t were removed from the site.

For the economic assessment, three different scenarios were evaluated. First one consisted on the excavation of the sediment and the transfer to the hazardous waste landfill. The cost of this operation was estimated on 28.6 M€, thus the unit cost was 55€/m^3. For the second scenario, the application of magnetic separation and the transfer of the magnetic fraction (contaminated material) to a hazardous waste landfill is taken into account. The application of magnetic separators could reduce the polluted sediment mass 4 times at least, which means less than 120,000 t of polluted sediment. For the operating costs of the physical separation, a treatment plant with a capacity of 500 tonnes per day supposes 10 €/t approximately (Drobe et al., 2021). Therefore, operating cost for the mineralurgical proccess is expected on 4.7 M€. This cost could be drastically increased due to milling or sieving processes, but according to grain-size distribution, it should not be necessary for this case. This estimation is in accordance with other soil washing approaches performed in EEUU and Belgium using magnetic separation for cleaning soils with similar capacity (NATO/CCMS, 1998;

NJDEP, 2001). Furthermore, according to the unit cost for transferring the 120,000 t of magnetic fraction to the landfill, the operating cost would increase to 11.9 M€ (4.7 + 7.2 M€). However, for the third scenario it was hypothesized that the Zn recovery could be performed from the magnetic fraction in the framework of the circular economy context. Assuming an average concentration of 2% Zn, the mass of Zn in the magnetic fraction would be 2400 t. For decreasing the operating costs, it is expected that Zn smelter close to the site could process these material, achieving the Zn recovery of 55% at least. In this sense, the cost of transportation and transfer to the landfill would be decrease to 7 M€, decreasing the total operating cost to 11.7 Mt. The economical benefit of Zn recovery would depend on the market price and the operating costs for the metallurgical processes performed by the Zn smelter.

According to the three scenarios, the application of magnetic separation for reducing the polluted sediment volume drastically impacts on the operating cost of the restoration approach. The reprocessing of Zn at the Zn smelter also decreases the operating cost, although the analysis of the metallurgical process needs to be addressed.

4. Conclusions

Affected coastal areas represent a major concern from an environmental point of view, which eventually will need to be solved. One of the most urgent problems is aroused by dredging activities, which are crucial for the proper maintenance of ports and bays and that generate high amounts of sediments considered toxic wastes due to the presence of metals and other pollutants. To solve this problem, these sediments can be transformed from waste to valuable resources by the application of magnetic separation.

Arsenic and metals, such as Cu, Pb, and Zn, were recovered from sediments taken in a highly impacted area using a wet high-intensity magnetic separator. Pollutants were concentrated in a small portion of the sediment due to the ferro- and paramagnetic properties of the polluted sediment particles. These properties were assessed by magnetic measurements. On the other hand, non-magnetic particles, mainly quartz, were also encountered in large amounts and with no pollutants. Therefore, the advantage of the method is twofold: Zn-enriched particles detected in the magnetic fraction can be subjected to metallurgical processes for Zn recovery, and unpolluted sediments can be reused as a valuable material for multiple uses, such as filling or construction materials.

For the economic assessment, three scenarios were defined to evaluate the impact of magnetic separation on the restoration of the site. The cost of the usual excavation, transfer and deposit on hazardous waste landfill approach would be reduced from 28.6 M€ to 11.9 M€ by the application of magnetic separation for decreasing the volume of polluted sediment. The reprocessing of magnetic fraction at the Zn smelter would reduce the operating costs on 0.2 M€. In this sense, future work will focus on reproducing the technology on a larger scale, coupled to hydrometallurgical processes, to evaluate if the promising results obtained in this work would be economically feasible in industrial applications.

Author contributions statement

Diego Baragaño: Conceptualization, Investigation, Formal analysis, Writing – original draft. **Edgar Berrezueta**: Investigation, Formal analysis, Writing – review & editing. **Michael Komárek**: Investigation, Writing – review & editing. **Juan María Menéndez Aguado**: Investigation, Writing – review & editing, Funding acquisition.

Declaration of competing interest

The authors declare that they have no known competing financial interests or personal relationships that could have appeared to influence the work reported in this paper.

Data availability

Data will be made available on request.

Acknowledgements

We would like to thank the Electron Microscopy Unit, Fluorescence and Electron Microprobe Unit, X-Ray Diffraction Unit and Magnetic Measurements Unit of the University of Oviedo for technical support. Diego Baragaño would like to thank the European Union-NextGenerationEU, Ministerio de Universidades, and Plan de Recuperación, Transformación y Resiliencia, through a call of the Universidad de Oviedo for the Postdoctoral grant (Ref. MU-21-UP2021-030 32892642). Tímea Kovács is thanked for her review of the English in the manuscript.

Appendix A. Supplementary data

Supplementary data to this article can be found online at https://doi.org/10.1016/j.jenvman.2023.117884.

References

Akcil, A., Erust, C., Ozdemiroglu, S., Fonti, V., Beolchini, F., 2015. A review of approaches and techniques used in aquatic contaminated sediments: metal removal and stabilization by chemical and biotechnological processes. J. Clean. Prod. 86, 24–36. https://doi.org/10.1016/J.JCLEPRO.2014.08.009.

Anbuselvan, N., , D., S.N., Sridharan, M., 2018. Heavy metal assessment in surface sediments off Coromandel Coast of India: implication on marine pollution. Mar. Pollut. Bull. https://doi.org/10.1016/j.marpolbul.2018.04.074.

Baragaño, D., Ratié, G., Sierra, C., Chrastny, V., Komárek, M., Gallego, J.R., 2022. Multiple pollution sources unravelled by environmental forensics techniques and multivariate statistics. J. Hazard Mater. 424, 127413.

Baragaño, D., Gallego, J.L.R., María Menéndez-Aguado, J., Marina, M.A., Sierra, C., 2021. As sorption onto Fe-based nanoparticles and recovery from soils by means of wet high intensity magnetic separation. Chem. Eng. J. 408, 127325 https://doi.org/10.1016/J.CEJ.2020.127325.

Cauwenberg, P., Verdonckt, F., Maes, A., 1998. Flotation as a remediation technique for heavily polluted dredged material. 1. A feasibility study. Sci. Total Environ. 209, 113–119. https://doi.org/10.1016/S0048-9697(98)80102-2.

CCME, 2001. Canadian Water Quality Guidelines for the Protection of Aquatic Life: CCME Water Quality Index 1.0. Canadian Water Quality Guidelines for the Protection of Aquatic Life.

Chen, L., 2011. Effect of magnetic field orientation on high gradient magnetic separation performance. Miner. Eng. 24, 88–90. https://doi.org/10.1016/j.mineng.2010.09.019.

CMAOTI, 2006. Decreto 81/2006, de 29 de junio, de la Consejería de medio ambiente, ordenación del territorio e infraestructuras. Boletín Oficial del Principado de Asturias del 21 de julio de 2006.

Crocetti, P., González-Camejo, J., Li, K., Foglia, A., Eusebi, A.L., Fatone, F., 2022. An overview of operations and processes for circular management of dredged sediments. Waste Manag. 146, 20–35. https://doi.org/10.1016/j.wasman.2022.04.040.

Dermont, G., Bergeron, M., Mercier, G., Richer-Laflèche, M., 2008. Soil washing for metal removal: a review of physical/chemical technologies and field applications. J. Hazard Mater. 152, 1–31. https://doi.org/10.1016/J.JHAZMAT.2007.10.043.

Drobe, M., Haubrich, F., Gajardo, M., Marbler, H., 2021. Processing tests, adjusted cost models and the economies of reprocessing copper mine tailings in Chile. Metals 11, 103. https://doi.org/10.3390/met11010103.

Fernández, B., Lara, L.M., Menéndez-Aguado, J.M., Ayala, J., García-González, N., Salgado, L., Colina, A., Gallego, J.L.R., 2020. A multi-faceted, environmental forensic characterization of a paradigmatic brownfield polluted by hazardous waste containing Hg, As, PAHs and dioxins. Sci. Total Environ. https://doi.org/10.1016/j.scitotenv.2020.138546.

Flor-Blanco, G., Flor, G., Pando, L., 2013. Evolution of the Salinas-El Espartal and Xagó beach/dune systems in north-western Spain over recent decades: evidence for responses to natural processes and anthropogenic interventions. Geo Mar. Lett. https://doi.org/10.1007/s00367-012-0301-3.

Forján, R., Baragaño, D., Boente, C., Fernández-Iglesias, E., Rodríguez-Valdes, E., Gallego, J.R., 2019. Contribution of fluorite mining waste to mercury contamination in coastal systems. Mar. Pollut. Bull. 149, 110576 https://doi.org/10.1016/J.MARPOLBUL.2019.110576.

Gallego, J.L.R., Ordóñez, A., Loredo, J., 2002. Investigation of trace element sources from an industrialized area (Avilés, northern Spain) using multivariate statistical methods. Environ. Int. 27, 589–596. https://doi.org/10.1016/S0160-4120(01)00115-5.

Gao, M., Sun, Q., Wang, J., Ding, S., 2021. Investigation of the combined use of capping and oxidizing agents in the immobilization of arsenic in sediments. Sci. Total Environ. 782, 146930 https://doi.org/10.1016/J.SCITOTENV.2021.146930.

Interstate Technology and Regulatory Council (ITRC), 1997. Technical and Regulatory Guidelines for Soil Washing, Metals in Soils Work Team. Washington, DC.

Julivert, M., Truyols, J., Marcos, A., Arboleya, M.L., 1973. MAGNA 50 (2ª Serie). Hoja 13 –Avilés. Instituto Geológico y Minero de España, Madrid.

Jha, D.K., Ratnam, K., Rajaguru, S., Dharani, G., Devi, M.P., Kirubagaran, R., 2019. Evaluation of trace metals in seawater, sediments, and bivalves of Nellore, southeast coast of India, by using multivariate and ecological tool. Mar. Pollut. Bull. https://doi.org/10.1016/j.marpolbul.2019.05.044.

Kennish, M.J., 2017. Estuaries: Anthropogenic Impacts. Springer, Cham, pp. 1–9. https://doi.org/10.1007/978-3-319-48657-4_140-2.

Kennish, M.J., 2002. Environmental threats and environmental future of estuaries. Environ. Conserv. https://doi.org/10.1017/S0376892902000061.

Kyllönen, H., Pirkonen, P., Hintikka, V., Parvinen, P., Grönroos, A., Sekki, H., 2004. Ultrasonically aided mineral processing technique for remediation of soil contaminated by heavy metals. Ultrason. Sonochem. 11, 211–216. https://doi.org/10.1016/J.ULTSONCH.2004.01.024.

Li, X., Zhang, J., Gong, Y., Liu, Q., Yang, S., Ma, J., Zhao, L., Hou, H., 2020. Status of copper accumulation in agricultural soils across China (1985–2016). Chemosphere. https://doi.org/10.1016/j.chemosphere.2019.125516.

Li, D., Yu, R., Chen, J., Leng, X., Zhao, D., Jia, H., An, S., 2022. Ecological risk of heavy metals in lake sediments of China: a national-scale integrated analysis. J. Clean. Prod. 334, 130206 https://doi.org/10.1016/j.jclepro.2021.130206.

Liu, J., Wei, X., Zhou, Y., Tsang, D.C.W., Bao, Z., Yin, M., Lippold, H., Yuan, W., Wang, J., Feng, Y., Chen, D., 2020. Thallium contamination, health risk assessment and source apportionment in common vegetables. Sci. Total Environ. https://doi.org/10.1016/j.scitotenv.2019.135547.

Meegoda, J.N., Perera, R., 2001. Ultrasound to decontaminate heavy metals in dredged sediments. J. Hazard Mater. 85, 73–89. https://doi.org/10.1016/S0304-3894(01)00222-9.

Mossinger, J., White, M., Goymer, P., 2013. Coastal regions. Nature. https://doi.org/10.1038/504035a.

Mulligan, Catherine N., Yong, R.N., Gibbs, B.F., 2001a. An evaluation of technologies for the heavy metal remediation of dredged sediments. J. Hazard Mater. 85, 145–163. https://doi.org/10.1016/S0304-3894(01)00226-6.

Mulligan, C.N., Yong, R.N., Gibbs, B.F., 2001b. Surfactant-enhanced remediation of contaminated soil: a review. Eng. Geol. 60, 371–380. https://doi.org/10.1016/S0013-7952(00)00117-4.

Negral, L., Suárez-Peña, B., Zapico, E., Fernández-Nava, Y., Megido, L., Moreno, J., Marañón, E., Castrillón, L., 2020. Anthropogenic and meteorological influences on PM10 metal/semi-metal concentrations: implications for human health. Chemosphere 243, 125347. https://doi.org/10.1016/j.chemosphere.2019.125347.

Norén, A., Karlfeldt Fedje, K., Strömvall, A.M., Rauch, S., Andersson-Sköld, Y., 2020. Integrated assessment of management strategies for metal-contaminated dredged sediments – what are the best approaches for ports, marinas and waterways? Sci. Total Environ. 716, 135510 https://doi.org/10.1016/J.SCITOTENV.2019.135510.

North Atlantic Treaty Organization's Committee on the Challenges of Modern Society (NATO/CCMS), Evaluation of Demonstrated and Emerging Technologies for the Treatment and Clean up of Contaminated Land and Groundwater, Pilot Study, Phase II Final Report, 1998. NATO, Brussels, Belgium. Number 219.

New Jersey Department of Environmental Protection (NJDEP), 2001. Certification Report for New Jersey Corporation for Advanced Technology (NJACT) Verification of Brice Environmental Services Corporation. Soil Washing Process).

Nukazawa, K., Itakiyo, T., Ito, K., Sato, S., Oishi, H., Suzuki, Y., 2021. Mineralogical fingerprinting to characterize spatial distribution of coastal and riverine sediments in southern Japan. Catena 203, 105323. https://doi.org/10.1016/j.catena.2021.105323.

Pell, R., Tijsseling, L., Goodenough, K., Wall, F., Dehaine, Q., Grant, A., Deak, D., Yan, X., Whattoff, P., 2021. Towards sustainable extraction of technology materials through integrated approaches. Nat. Rev. Earth Environ. 2, 665–679. https://doi.org/10.1038/s43017-021-00211-6.

Peng, J. feng, Song, Y. hui, Yuan, P., Cui, X. yu, Qiu, G. lei, 2009. The remediation of heavy metals contaminated sediment. J. Hazard Mater. 161, 633–640. https://doi.org/10.1016/J.JHAZMAT.2008.04.061.

Sierra, C., Boado, C., Saavedra, A., Ordóñez, C., Gallego, J.R., 2014a. Origin, patterns and anthropogenic accumulation of potentially toxic elements (PTEs) in surface sediments of the Avilés estuary (Asturias, northern Spain). Mar. Pollut. Bull. https://doi.org/10.1016/j.marpolbul.2014.06.052.

Sierra, C., Martínez-Blanco, D., Blanco, J.A., Gallego, J.R., 2014b. Optimisation of magnetic separation: a case study for soil washing at a heavy metals polluted site. Chemosphere 107, 290–296. https://doi.org/10.1016/J.CHEMOSPHERE.2013.12.063.

Wang, L., Chen, L., Tsang, D., Li, J., Hou, D., Ding, S., Poon, C., 2018. Recycling dredged sediment into fill materials, partition blocks, and paving blocks: technical and economic assessment. J. Clean. Prod. 199, 69–76. https://doi.org/10.1016/j.jclepro.2018.07.165.

Wills, B.A., Napier-Munn, T.J., 2006. Mineral Processing Technology: an Introduction to the Practical Aspects of Ore Treatment and Mineral Recovery, seventh ed. Butterworth-Heinemann, Burlington, MA.

Wu, W., Wu, P., Yang, F., Sun, D. ling, Zhang, D.X., Zhou, Y.K., 2018. Assessment of heavy metal pollution and human health risks in urban soils around an electronics manufacturing facility. Sci. Total Environ. https://doi.org/10.1016/j.scitotenv.2018.02.183.

Xu, D., Fu, R., 2022. Mechanistic insight into the release behavior of arsenic (As) based on its geochemical fractions in the contaminated soils around lead/zinc (Pb/Zn) smelters. J. Clean. Prod. 363, 132348 https://doi.org/10.1016/j.jclepro.2022.132348.

Xu, J., Bravo, A.G., Lagerkvist, A., Bertilsson, S., Sjöblom, R., Kumpiene, J., 2015. Sources and remediation techniques for mercury contaminated soil. Environ. Int. https://doi.org/10.1016/j.envint.2014.09.007.